Supporting Information for "Comparing observations and parameterizations of ice-ocean drag through an annual cycle across the Beaufort Sea"

Samuel Brenner [1], Luc Rainville [1], Jim Thomson [1], Sylvia Cole [2], Craig Lee [1]

[1] Applied Physics Laboratory, University of Washington, Seattle, WA, USA

[2] Woods Hole Oceanographic Institution, Woods Hole, MA, USA

Contents of this file

1. Text S1 to S2

2. Figures S1 to S4

3. Table S1

Introduction This supporing information provides additional figures and tables and discusses the sensitivity of the results of the main study.

Text S1. *Sensitivity of results: geostrophic velocity*

The inclusion of the geostrophic velocity, $\boldsymbol{u}_g$ in eq. (3) arises from sea surface tilt in the sea ice momentum equation, and the assumption of geostrophic balance: $f\hat{k} \times \boldsymbol{u}_g = g\nabla\eta$. However, there is some ambiguity involved in defining a geostrophic velocity from ADCP-measured ocean velocity profiles. For the present study, $\boldsymbol{u}_g$ is based on the measured velocity averaged over some depth range, which has previously been found to be in good agreement with estimates of sea surface height from satellite altimetry on monthly timescales

---

November 13, 2020, 12:52am

(Armitage et al., 2017). Over a 12-year record in the Beaufort Sea, Armitage et al. (2017) found that the 5 m to 20 m depth range produced the best match between monthly averaged velocities and satellite altimetry estimates of geostrophic velocity. Other studies have used different depth ranges. For example, Randelhoff, Sundfjord, and Renner (2014) used an average velocity in the 17 m to 22 m depth range to represent the undisturbed ocean beneath sea ice and Cole et al. (2017) define a geostrophic reference velocity in reference to the depth of the mixed-layer. For consistency with Armitage et al. (2017), we define $\boldsymbol{u}_g$ as the average velocity from 5 m to 20 m depth low-pass filtered with a 2-day cut-off (to reflect that the geostrophic balance adjustment occurs over inertial timescales).

The values of $\boldsymbol{\tau}_{io}$ and C_{io} are fairly insensitive to the choice of averaging depth used to define the geostrophic velocity. Averaged through the full record, ice-ocean and atmosphere-ice stresses almost perfectly balance (table S1 and fig. S2). The Coriolis acceleration term is $\sim$3–4% of $\boldsymbol{\tau}_{io}$, but it largely cancelled by local acceleration and sea surface tilt. These results are generally consistent with those by Steele, Zhang, Rothrock, and Stern (1997), who also find a minimal contribution from Coriolis and tilt terms (their model neglected local acceleration). While different choices of the depth range used for averaging in the definition of $\boldsymbol{u}_g$ result in different relative contributions to the ice-ocean stress (table S1), these amount to differences in $\boldsymbol{\tau}_{io}$ on the order of $\sim$1–2% and aren't substantial enough to impact the calculated values of C_{io}.

Text S2. *Sensitivity of results: atmosphere-ice drag coefficient*

As the ice-ocean stress in free-drift conditions is largely set by the atmosphere-ice stress (table S1 and fig. S2), the values of $\boldsymbol{\tau}_{io}$ and consequently C_{io} will be sensitive to the atmosphere-ice stress. The atmospheric stress available from the ERA5 re-analysis prod-

uct represents the total effective stress $\boldsymbol{\tau}_{atm}$ (eq. 4b) over a grid cell in mixed ice and open-water conditions. To partition stress appropriately for eq. (3), it is necessary to calculate the atmosphere-ice stress component, which is done using the quadratic drag law, eq. (1b), which relies on the atmosphere-ice drag coefficient, C_{ai}. For consistency with the ERA5 re-analysis product that we use for wind speed, we calculate the neutral C_{ai} using the formulation from the European Centre for Medium-Range Weather Forecasts (ECMWF) model: $C_{ai} = [\kappa/\ln(z_{ref}/z_0)]$, with $z_{ref} = 10\,\mathrm{m}$, and the surface roughness z_{0M} given as a function of ice concentration, A, by (ECMWF, 2019):

$$z_{0M} = 10^{-3} \times \max\left\{1, \quad 0.93(1 - A) + 6.05\exp[-17(A - 0.5)^2]\right\}. \tag{S1}$$

To test the sensitivity of calculated ice-ocean drag values to the parameterization of the atmosphere-ice drag coefficient, two alternative formulations of C_{ai} are considered: (1) constant drag; and (2) the drag parameterization by Lüpkes, Gryanik, Hartmann, and Andreas (2012). For constant drag, we use $C_{ai} = 1.47 \times 10^{-3}$ (based on a constant roughness length $z_{0M} = 2.3 \times 10^{-4}\,\mathrm{m}$, appropriate for winter Arctic conditions; Andreas, Persson, et al., 2010). The parameterization by Lüpkes et al. (2012) forms the basis for the ice-ocean drag parameterization by Tsamados et al. (2014) and is based on ice geometry characteristics; however, the authors provide a hierarchy of simplifications to the model based on empirical relationships found between ice morphology and concentration. To construct a C_{ai} only as a function of A based on Lüpkes et al. (2012) for the purpose of sensitivity testing, we use their eqs. 2 and 53–54 with h_f given by their eq. 25 and ignore the effects of melt ponds (consistent with Elvidge et al., 2016). Note that Lüpkes et al. (2012) parameterize the total neutral atmospheric drag coefficient: $C_{atm} = AC_{ai} + (1 - A)C_{ao}$; however, since the skin drag over open water in their formulation is equivalent to

the atmosphere-ocean drag coefficient (C_{ao}), we can determine C_{ai} explicitly. Compared with the ECMWF parameterization that is used in the ERA5 re-analysis product, these test cases give quite different forms of C_{ai} (fig. S3).

These three schemes have somewhat similar values of C_{ai} at 100% ice concentration (values vary from 1.47×10^{-3} to 1.98×10^{-3}); however, at low concentrations, the value of C_{ai} can more than double depending on the choice of parametrization scheme (values vary from 1.47×10^{-3} to 3.91×10^{-3}; fig. S3). Despite the much higher C_{ai} during the fall season when using the Lüpkes et al. (2012) parameterization (compared to ECMWF; fig. S4a), the observed seasonal variations in the ice-ocean drag coefficient exist regardless of the C_{ai} scheme used (fig. S4b). The differences between the fall minimum and winter maximum C_{io} are slightly muted when using the Lüpkes et al. (2012) scheme for C_{ai}, but enhanced when using a constant atmosphere-ice drag coefficient (due to lower values of C_{ai} during the fall). While the seasonal patterns of C_{io} are robust across different C_{ai} parameterization schemes, the values of C_{io} are impacted by the choice of scheme for C_{ai}. Annual average values of C_{io} taken across all three moorings are 4.6×10^{-3} when using the ECMWF parameterization for C_{ai} (**??**), 4.1×10^{-3} for the Lüpkes et al. (2012) param- eterization, and 3.3×10^{-3} for constant C_{ai}; these values directly reflect the proportional changes between C_{ai} calculated using the different parameterization schemes.

In testing these different parameterizations, we use the same wind speed for each. How- ever, that wind speed is provided by the ERA5 re-analysis, which implements the ECMWF parameterization for surface drag. If a different atmospheric drag parameterization was implemented in the re-analysis model, the wind speed would adjust accordingly (e.g., a lower surface drag may result in a higher wind speed). The change in wind speed might

partly offset the impacts of different C_{ai} values in setting $\boldsymbol{\tau}_{ai}$ and thus C_{io} for different parameterization schemes, so the overall sensitivity of C_{io} to choices of C_{ai} when accounting for associated wind speed variations may be lowered. Unfortunately, we are unable to test that effect.
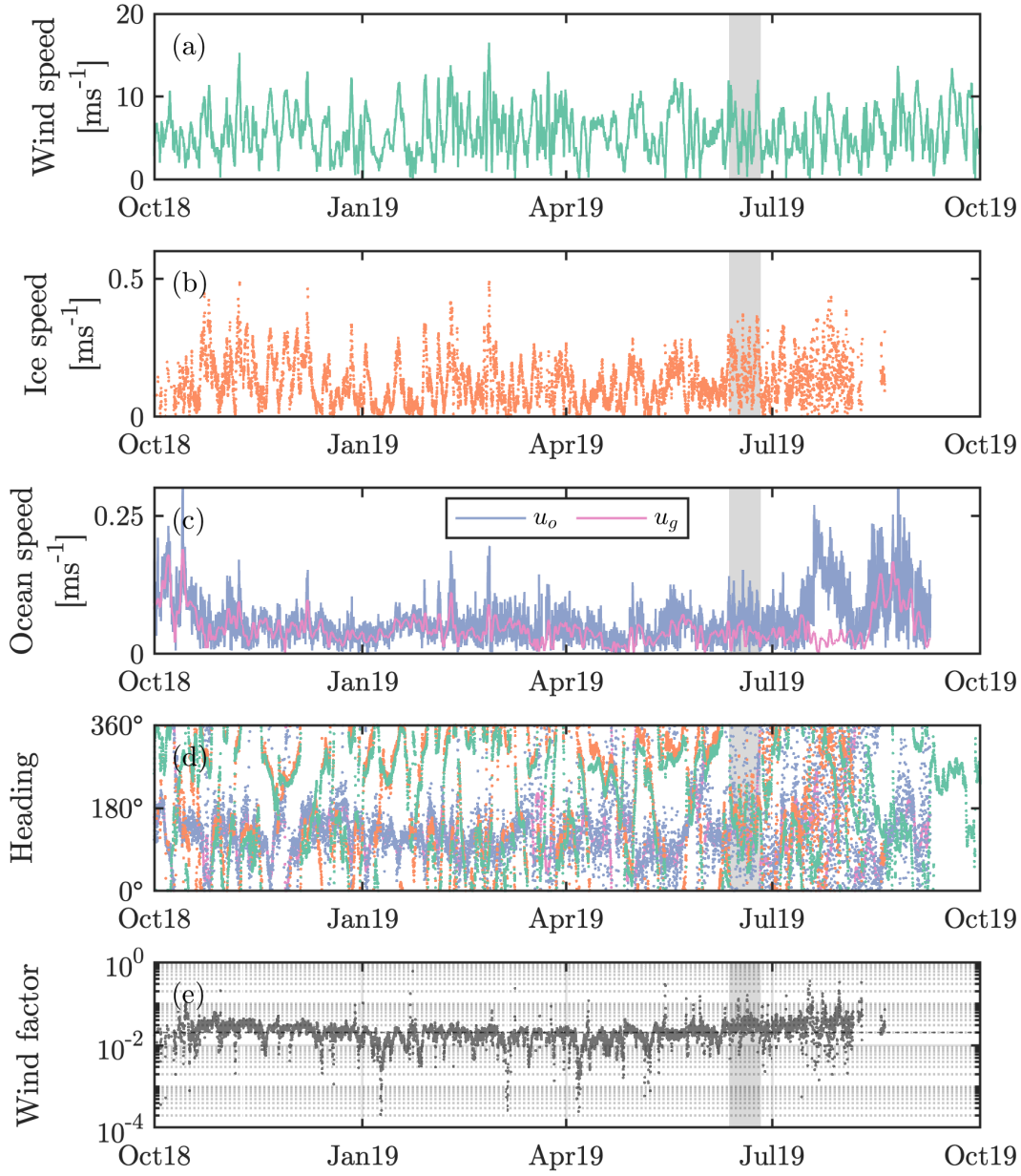
Figure S1. Hourly timeseries at SODA-B of (a) wind speed; (b) ice speed; (c) speed ocean current at 10-m reference depth ($\boldsymbol{u}_o$) and geostrophic current ($\boldsymbol{u}_g$); (d) directions for each of the speeds in (a-c), coloured correspondingly (using a conventions of the direction each velocity vector is pointing towards measured clockwise from North); (e) wind factor ($|\boldsymbol{u}_i|/|\boldsymbol{u}_a|$). The shaded grey background shows the time period used in fig. S2.

Table S1. Annual median values of the stress components of each of the terms in the sea ice momentum balance (eq. 3) projected onto the direction of $\boldsymbol{\tau}_{io}$. Different rows for the sea surface tilt component, $\rho_o d_i f \hat{k} \times \boldsymbol{u}_g$, (labelled 1–4) correspond to different depth-ranges used for averaging in the definition of $\boldsymbol{u}_g$: (1) 5 m to 20 m, used for the main text; (2) 17 m to 22 m; (3) the full depth profile measured by the ADCP; and (4) rather an a depth-averaged velocity, $\boldsymbol{u}_g$ is defined by the velocity in the deepest ADCP bin.

|	Projected stress [mPa]		
	SODA-A	SODA-B	SODA-C
$\boldsymbol{\tau}_{io}$	116.7	96.8	69.3
$\boldsymbol{\tau}_{ai}$	116.5	97.7	71.4
$-\rho_o d_i \frac{\partial \boldsymbol{u}_i}{\partial t}$	0.1	0.4	0.3
$-\rho_o d_i f \hat{k} \times \boldsymbol{u}_i$	-5.4	-2.7	-4.4
[(1)] $\rho_o d_i f \hat{k} \times \boldsymbol{u}_g$	5.0	1.5	1.5
[(2)] $\rho_o d_i f \hat{k} \times \boldsymbol{u}_g$	4.1	1.1	0.8
[(3)] $\rho_o d_i f \hat{k} \times \boldsymbol{u}_g$	3.6	0.9	1.3
[(4)] $\rho_o d_i f \hat{k} \times \boldsymbol{u}_g$	2.3	0.4	0.3
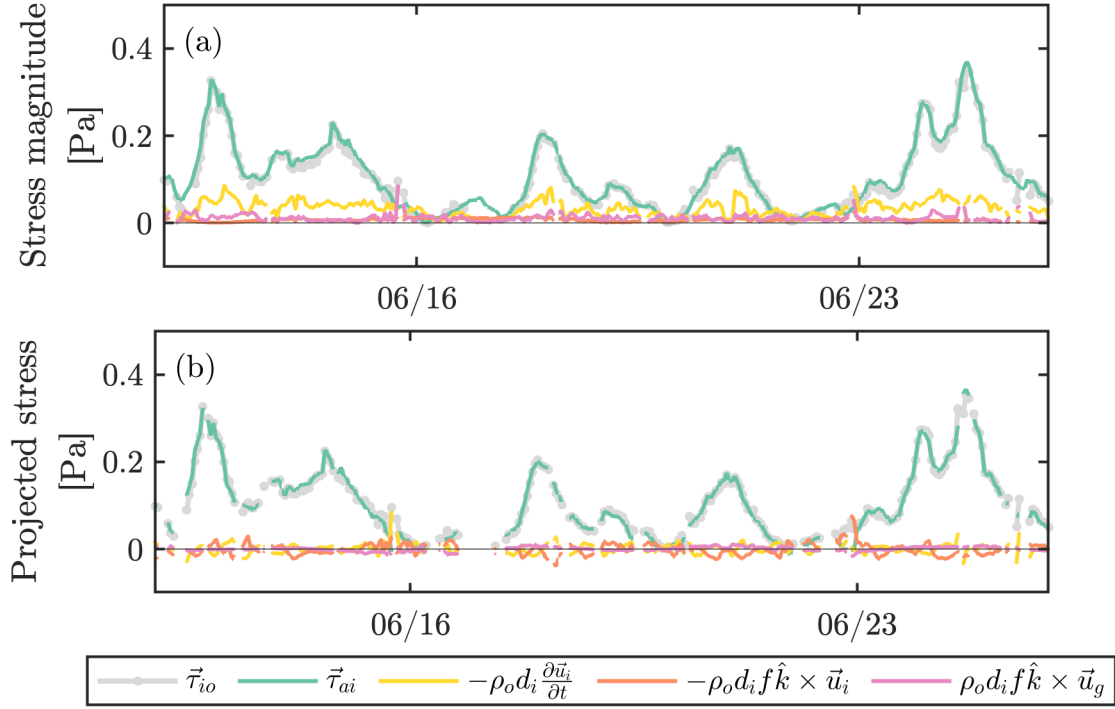
Figure S2. An example period from two week period in summer at SODA-B showing the size of different terms in the sea ice momentum balance (eq. 3): (a) magnitude of each stress component; (b) stress components projected onto the direction of $\boldsymbol{\tau}_{io}$. Missing values of $|\boldsymbol{\tau}_{io}|$ in (a) and of all stress components in (b) are due to the exclusion of $|\boldsymbol{\tau}_{io}|$ values when the wind factor is $< 2\%$.
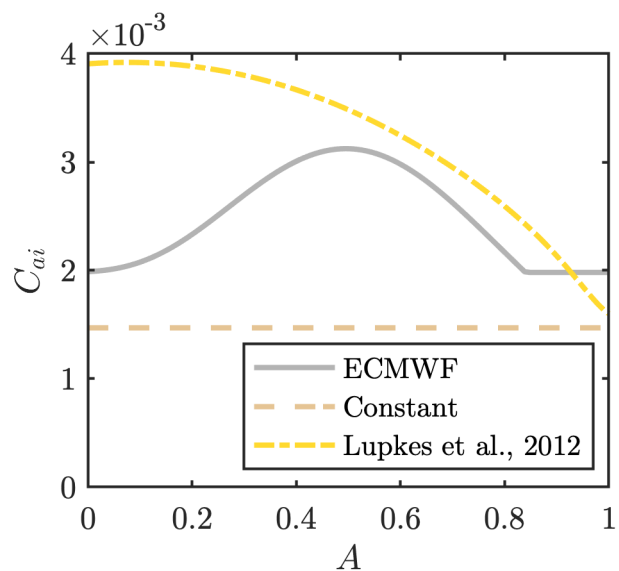
Figure S3. Parameterized atmosphere-ice drag coefficient, C_{ai}, as a function of sea ice concentration, A.

:
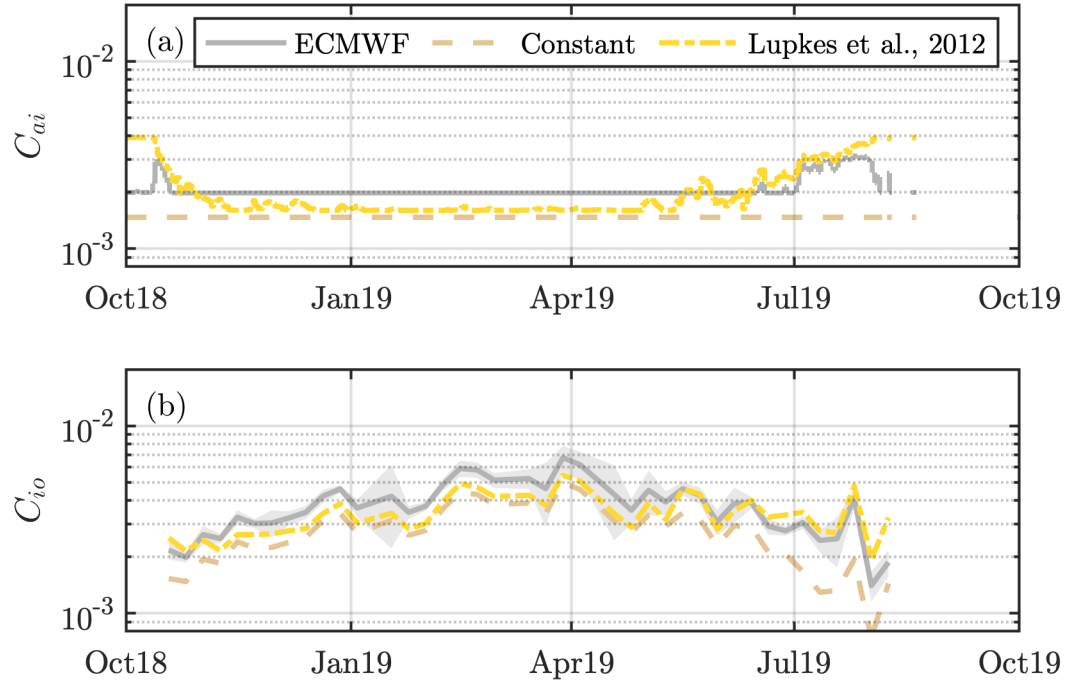
Figure S4. Timeseries at SODA-B of (a) atmosphere-ice drag coefficients, C_{ai}, calculated using different parameterization schemes, and (b) corresponding ice-ocean drag coefficients, C_{io}. The grey-shaded region in (b) shows the 95% uncertainty range associated with regression procedure to determine C_{io} when C_{ai} is calculated with the ECMWF scheme.